Neoplasia • Vol. 5, No. 6, November/December 2003, pp. 546–554 546

www.neoplasia.com

High-Resolution Longitudinal Screening with Magnetic Resonance Imaging in a Murine Brain Cancer Model

Nicholas A. Bock[*,†,1], *Gelareh Zadeh*[‡,§,1], *Lori M. Davidson*[†], *Baoping Qian*[‡], *John G. Sled*[*,†], *Abhijit Guha*[‡,§] *and R. Mark Henkelman*[*,†]

*Department of Medical Biophysics, University of Toronto, Toronto, Canada; [†]Mouse Imaging Center (MICe), Hospital for Sick Children, Toronto, Canada; [‡]Arthur and Sonia Labatt Brain Tumor Center, Hospital for Sick Children, University of Toronto, Toronto, Canada; [§]Division of Neurosurgery, Western Hospital, University of Toronto, Toronto, Canada

Abstract

One of the main limitations of intracranial models of diseases is our present inability to monitor and evaluate the intracranial compartment noninvasively over time. Therefore, there is a growing need for imaging modalities that provide thorough neuropathological evaluations of xenograft and transgenic models of intracranial pathology. In this study, we have established protocols for multiple-mouse magnetic resonance imaging (MRI) to follow the growth and behavior of intracranial xenografts of gliomas longitudinally. We successfully obtained weekly images on 16 mice for a total of 5 weeks on a 7-T multiple-mouse MRI. T2- and T1-weighted imaging with gadolinium enhancement of vascularity was used to detect tumor margins, tumor size, and growth. These experiments, using 3D whole brain images obtained in four mice at once, demonstrate the feasibility of obtaining repeat radiological images in intracranial tumor models and suggest that MRI should be incorporated as a research modality for the investigation of intracranial pathobiology.

Neoplasia (2003) **5**, 546–554

Keywords: Multiple-mouse magnetic resonance imaging, intracranial tumor models, microcomputed tomography, gliomas, preclinical screening.

Introduction

Preclinical models of human diseases are vital for basic and translational research, and an increasing number of specific and genetically targeted spontaneous transgenic intracranial glioma models are being developed [1] and added to the established orthotopic xenograft models of intracranial tumors. An important model for studying central nervous system (CNS) tumors is in the intracranial microenvironment, as the brain has several unique and critical physiological attributes such as the blood–brain barrier (BBB), vascularity, and extracellular matrix (ECM). Orthotopic intracranial models of brain tumors provide complimentary information to that obtained from subcutaneous xenograft models of brain cancer. Direct monitoring and evaluation of the intracranial compartment, however, is not readily possible. Therefore, there is a growing need for imaging modalities used for screening that provide thorough neuropathological evaluations of xenograft and transgenic models of intracranial pathology.

Magnetic resonance imaging (MRI) is adept at investigating intracranial models of brain cancer and is the best method of following *in vivo* tumor growth longitudinally. Similar to the established clinical role of MRI in the diagnosis and follow-up of CNS neoplasia, small animal MRI is becoming established as a research tool to image intracranial tumor models. MRI can follow them longitudinally with accurate spatial localization to ultimately develop more sensitive methods for characterizing intracranial tumors and answer biological questions related to their pathogenesis [2–5]. In addition to fundamental parameters such as tumor size, shape, and pattern of growth, small animal MRI has the potential to monitor physiological parameters such as edema, invasion, angiogenesis, and responses to various potential therapeutic interventions. To date, the study numbers have been small because long imaging times are needed to obtain high-resolution 3D images over the whole brain in mice, even at high magnetic field strengths. The linear scaling factor between mouse and human brain structures is about 10; therefore, better the image resolution is required in order to obtain images in a mouse brain that compare in the level of structural detail to those of a human brain. For example, a human clinical image with an in-plane resolution of 1 × 1 mm and a slice thickness of 5 mm would correspond to an in-plane resolution of 100 × 100 μm and a slice thickness of 500 μm in an image of a mouse. A thorough screen should include a relatively large number of animals to assess biological heterogeneity and it is important that the throughput of MRI is improved.

In the simplest case, an MRI screen should measure tumor take, location, and growth rate over the survival period of the

Address all correspondence to: Abhijit Guha, MD, FACS, FRCSC, 4W-446 Western Hospital, 399 Bathurst Street, Toronto, Ontario, Canada M5T 2S8. E-mail: abhijit.guha@uhn.on.ca

[1]Both authors have made equal contributions to this work.

Received 24 July 2003; Revised 17 September 2003; Accepted 24 September 2003.

model. The data gathered from an MRI screen can provide information to characterize the models, such as tumor location, the latency of tumor take, and anatomical limits of tumor growth. This baseline information is essential for planning future detailed MRI and histological studies, in addition to testing the efficacy of therapeutic compounds. The screen should also be noninvasive to minimize the impact of the MRI procedure on the outcome of the study.

The difficulty, however, in using MRI for initial screening is that, currently, very little is known about the MRI appearance and behavior of intracranial tumor models in mice. Recent reports show that different cell lines grown as intracranial tumors can generate variable MRI signal appearances in mouse tumors that also differ from the appearance of human tumors seen in clinical MRI [3]. The differences in signal are expected, as various astrocytoma cell lines will generate tumors of variable genotype, phenotype, and histopathology. This is a rapidly evolving field of research and future studies will need to focus on establishing and characterizing the underlying mechanisms of variability in MRI appearance between various cell lines used to generate different intracranial xenograft models, because this information is important to allow accurate use of the models in imaging studies. It should also be kept in mind that, to date, mouse imaging studies are performed over a range of different MRI field strengths, which further confounds the interpretation of image contrast seen between different cell lines. Therefore, a reasonable MRI survey screen that has a good temporal resolution over the course of mouse survival is needed for tumor models and accounts for possible tumor contrast mechanisms with appropriately weighted imaging sequences (notably T2-weighted, T1-weighted, and T1-weighted with contrast agent enhancement). Such a screen should also image the entire brain at a resolution that is diagnostically comparable to human clinical MRI.

In order to fulfill the above requirements for studying both orthotopic xenograft and transgenic models of intracranial gliomas, we have performed an MRI screen in an orthotopic xenograft model of astrocytoma to test a protocol for screening larger numbers of tumor-bearing mice. This preliminary study had the technical goal of establishing an MRI screen to characterize intracranial tumors and to guide future studies. The model is based on an intracranial injection of the established human malignant astrocytoma cell line U87 into NODSCID mice. We also examined the use of MRI to evaluate an altered physiological parameter; we used U87 cells with an altered expression of angiopoietins, an important angiogenic cytokine family that we have shown to play a significant role in regulating the vascularity and growth of astrocytoma xenograft models (submitted for publication). Angiopoietin-1 (Ang1) increases tumor vascularity and confers growth advantage to tumors, whereas Angiopoietin-2 (Ang2) generates abnormal tumor vascularity without altering tumor growth. Ultimately, our objective is to determine the effect of angiopoietins on tumor latency, tumor growth, and vascularity using weekly longitudinal MRI, followed by histology and microcomputed tomography (micro-CT). In this study, we followed a total of 16 mice—four mice from each of three groups (control tumor, Ang1 upregulated tumor, and Ang2 upregulated tumor) plus a cohort of four age-matched mice without tumors—over the 5-week survival curve for the model to identify tumors with MRI and follow them longitudinally. To properly characterize the tumors, we imaged the whole brain with contiguous 2D multislice and 3D MRI sequences to avoid the difficulty of 2D slices missing foci or whole tumors. In general, the time needed for high-resolution 3D imaging further limits the throughput of MRI, but we were able to increase throughput in our study by using our multiple-mouse MRI technique [6] to image groups of four mice simultaneously. Extending our technique to image a greater number of mice will enable high-throughput, high-resolution serial screening with MRI in a variety of xenograft and transgenic mouse models of brain cancer. The study is an example of a typical mouse cancer MRI screen utilizing 3D whole brain images and spotlights the excellent sensitivity of MRI for following lesions longitudinally *in vivo*.

Materials and Methods

Cells and Reagents

Established U87 MG human astrocytoma cells were obtained from the American Type Culture Collection (ATCC; Rockville, MD) and maintained in Dulbecco's minimal essential medium (DMEM; Cellgro, Herndon, VA) supplemented with 10% FBS and penicillin–streptomycin antibiotics. Full-length human *ANG1* and *ANG2* cDNA (a gift from K. Alitalo, Helsinki, Finland) were subcloned into the pSec vector (Invitrogen, Carlsbad, CA) to allow generation of Myc-Histidine epitope-tagged constructs. The Ang-Myc/HIS sequence was subcloned into the *Bam*HI and *Eco*RI sites of a pCAGG vector that contains a CMV promoter with a chicken β-actin enhancer. Stable cell lines were generated by transfection of the vector "pCAGG-Ang-Myc/HIS-Zeocin" into the U87 cell line using Lipofectamine 2000 (Gibco/BRL, Gaithersburg, MD) as per the manufacturer's instructions. Twenty stable clones, selected with 1 mg/ml Zeocin (Invitrogen), were examined for Ang1 and Ang2 expression by Western blot analysis. Two single clones with the highest expression of Ang1 above baseline parental levels as well as one pooled clone of Ang1 were selected. Similarly, for Ang2, one single clone and one pooled clone with the strongest expression were selected. For control clones, empty vector transfectants were used.

Animals

All of the mice used in this study were maintained under protocols approved by the Hospital for Sick Children, Toronto. For the orthotopic astrocytoma model, established human astrocytoma cells U87 (10^6 cells in DMEM media) were implanted using a rodent stereotactic frame and a Hamilton syringe 3 mm deep into the frontal cortex of NODSCID mice. Stable U87 cell lines overexpressing either Ang1 or Ang2 were injected similarly. For each of the three cell types (U87 parental cell line for control tumors, U87 Ang1 upregulated cell line, and U87 Ang2 upregulated cell line)

four mice were generated. Another four mice without cell implantation were used as normal brain controls. The animals were followed clinically and when they exhibited symptoms consistent with failure to thrive as per animal care protocols, they were sacrificed by perfusion fixation with BrDU after an intravenous injection of 2% Evans Blue solution (2 ml/kg) to analyze BBB status and vessel permeability. The time interval between the injection of Evans Blue and the perfusion and killing of mice was approximately 30 minutes. The brains were dissected and placed in formalin for histopatholgical analysis.

MRI

MRI was performed on a 7-T scanner (Varian, Palo Alto, CA) outfitted with four parallel receivers for multiple-mouse imaging. Four mice were imaged together with an array of four many-runged 3-cm inner diameter birdcage coils of Varian's Millipede design [7]. The imaging consisted of T2- and T1-weighted sequences with a field-of-view (FOV) covering the entire brain. The mice were mechanically positioned in the scanner to obviate the need for scout scans to locate their brains. Screening started 2 weeks after cell injection with a T2-weighted sequence and continued every week for 3 weeks. The T2-wieghted sequence was replaced at week 4 with a weekly T1-weighted sequence that continued until the mice failed to thrive and were sacrificed. The T2-weighted sequence was a multislice spin-echo sequence with the slices placed in the coronal direction in the brain [repetition time (TR) = 3000 milliseconds, echo time (TE) = 30 milliseconds, FOV: readout $\times$ phase = 512 $\times$ 128 = 80 $\times$ 20 mm, slice thickness = 0.5 mm, number of averages (NEX) = 6, total imaging time = 38 minutes]. Because the TR needs to be several seconds long to produce T2 weighting in the mouse brain [8], a multislice sequence with contiguous slices was used instead of a 3D sequence to reduce the imaging time. The T1-weighted sequence used a 3D spin-echo sequence with the best resolution in the horizontal plane (TR = 300 milliseconds, TE = 10 milliseconds, Fov:readout $\times$ phase $\times$ phase = 256 $\times$ 128 $\times$ 32 = 40 $\times$ 20 $\times$ 16 mm, NEX =1, total imaging time = 21 minutes). The T1-weighted sequence was applied once without contrast, then again 20 minutes after a tail vein injection of 0.1 mM/kg gadopentetate dimeglumine contrast agent (Berlex, Lachine PQ). Temperature, electrocardiogram (ECG), and breathing rate in the four mice were monitored using a custom-built system. The mice were anesthesized during imaging with 1% isofluorane in O_2 delivered by nose cones, and were warmed with hot air to control their temperatures.

Histopathology

Fixed brains were paraffin-embedded, sectioned (4 μm), and examined histologically using hematoxylin and eosin (H&E) stains together with immunohistochemical staining for Factor VIII to mark endothelial cells. Histological examinations were performed on sections corresponding to the location of lesions seen on MRI.

Micro-CT

One mouse with a developed control U87 tumor was selected for micro-CT imaging of contrast agent–loaded vessels based on a T1-wieghted image with contrast agent enhancement. It was anesthesized by an intraperitoneal injection of ketamine (50 mg/kg) and xylazine (10 mg/kg). Following a 500-U subcutaneous injection of heparin, the mouse's chest was opened and another solution of heparin (1 U/ml) and physiologically buffered saline at 37° C was injected through the left ventricle and drained from the right atrium to replace the blood. This was followed by an infusion of Microfil MV-122 (Flow Tech Inc., Carver, MA), a silicone rubber compound with a viscosity initially comparable to blood, that begins to harden 30 minutes after injection. The brain was excised and stored at 4° C in a solution of 10% neutral-buffered formalin. The infused Microfil was allowed to cure over a period of 12 hours and was the source of contrast in the resulting micro-CT image. All fluids were infused at a constant pressure of 160 mm Hg (21.3 kPa) to preserve physiological vessel caliber.

A 3D CT data set was acquired for the excised brain using an MS-8 micro-CT scanner (GE Medical Systems, London, Ontario, Canada) (submitted for publication). With the X-ray source at 80 kVp (mean energy of incident beam: 32 keV), the image was acquired in 2.5 hours with 900 views and reconstructed using the Feldkamp algorithm [9] for cone beam CT geometry. The vasculature in the image was segmented using a simple thresholding algorithm and its surface was rendered. The computed image shows both arterial and venous vessels as highly intense regions of a signal against a relatively uniform background with a low signal. Regions where the contrast agent has leaked into the extravascular space also have a high signal intensity.

Results

Feasibility of Longitudinal MRI Studies

One purpose of this study was to determine the effect of our high-throughput MRI screen on the outcome and overall survival of the mice. The mice tolerated the 2-hour anesthetic period required for the entire MRI procedure well at each time point despite harboring large mass-occupying lesions in the brain. The pooled overall survival of tumor-bearing mice included in the MRI screen was (33 ± 1 days), which was the same as the survival of tumor-bearing mice not included in the MRI screen (36 ± 5 days). These results confirm and clearly demonstrate the feasibility of using MRI for follow-up of tumor growth in mouse models of intracranial tumors and that it is not detrimental to the outcome and survival of mice.

Tumor Characterization

A second purpose of this study was to determine if we could detect tumors using MRI over the course of survival of the mice and characterize the MRI appearance of these tumors. We began weekly imaging 2 weeks postimplantation using T2-weighted sequences as T2 sequences are often

used to delineate the extent of tumor mass and tumor-associated edema from normal brain tissues, although even clinically, the problem of delineating tumor mass from tumor-associated edema remains an unsolved problem. A technical advantage is that T2-weighted sequences require only one set of images and no intravenous injection of contrast agent (instead of two sets of images and an injection for the T1-weighted sequence). We used images from age-matched mice without tumors to distinguish lesions from normal anatomy in the images of tumor-bearing mice. Previous growth rate curves in a similar tumor model from conventional pathology [10] showed tumor take between weeks 2 and 3 postimplantation; thus, we chose week 2 as our first time point for imaging and followed the mice weekly for 3 weeks with T2-weighted images. We began T1-weighted imaging with and without contrast agent at week 5 to assess the extent of tumor vascularization and vessel permeability in the larger tumors at week 5. Table 1 summarizes the appearance of lesions during the screen in the tumor-bearing mice and Figure 1 shows the typical tumor appearance in one control U87 tumor mouse at each weekly time point. Hypointense lesions were seen in 7 of 11 mice on the first T2-weighted image (week 2). Endogenous tumor enhancement was not seen in any of the mice in the T1-weighted images; however, with injection of the contrast agent, eight of nine mice had lesion enhancement. The lesions detected on the MRI images were confirmed to be tumors by both Evans Blue demarcation and histology at necropsy for each mouse. We did not confirm whether the tail vein injection of the contrast agent was consistent in all of the mice; thus, one mouse that did not show lesion enhancement on its T1-weighted image might not have had an adequate concentration of gadolinium in its blood.

Tumor Variability

Tumor contrast arises in T1-weighted images following an injection of a gadolinium contrast agent because of the increased density of blood vessels in the tumor and because the agent leaks from tumor vessels that have a compromised BBB. Another technique that stains tumors with a compromised BBB and that can be used to see the extent of tumors in excised brains is an injection of Evans Blue dye. Figure 2*A* shows a photograph of a tumor stained with the established Evans Blue technique in the excised brain of a mouse and Figure 2*B* shows a T1-weighted MRI image with a volume-rendered region of contrast agent enhancement in the same mouse before it was sacrificed. The two methods are in good visual agreement, although the MRI provides a much better 3D characterization of the extent and location of the tumor and can be used to make accurate volume measurements. Figure 3 shows volume-rendered regions of enhancement in four tumor-bearing mice that were imaged together 5 weeks postinjection and reveals overall variability in the size and shape of individual tumors. The advantage of using a 3D MRI image over the whole brain is clear from Figure 3—the complex extent and precise margins of the tumors would be impossible to characterize in a single MRI slice and would be misrepresented if multiple slices that were not contiguous were used.

Table 1. Lesion Appearance on Week 2 T2-Weighted Images and on Week 5 T1-Weighted Images Following Administration of a Contrast Agent.

Lesion Appearance	Number of Mice
Hypointense only on T2	7/11
Hyperintense only on T2	1/11
Heterogeneous on T2	2/11
Hyperintense on T1 with contrast agent	8/9

All mice had confirmed tumors on histology.

Ventricle Size

In addition to characterizing tumor lesions, MRI can also be used to detect other neuropathological abnormalities that arise directly or indirectly as a result of the glioma that might be missed on histological evaluation alone. Because T2-weighted images show cerebrospinal fluid (CSF) and major brain structures well, they are good for identifying abnormalities in the brain [11]. An unexpected finding in our study was the presence of enlarged ventricles seen early and throughout the 5-week period of the study in all mice bearing Ang1 upregulated tumors (Figure 4). The ventricle dilatation was a pan-ventriculomegaly and no evidence of CSF obstruction or tumor growth in the ventricles was seen. As well, the dilatation was not related to tumor size, location, morphology, or pattern of tumor cell invasion. Additionally, ventriculomegaly was only seen with the Ang1 upregulated tumors and not seen in control or Ang2 upregulated tumors. This finding suggests that the dilatation of ventricles was related to the biological effects of Ang1—potentially an interference with CSF absorption. This was an interesting and unexpected finding that illustrates the strengths and benefits of whole brain imaging for intracranial tumor models and also reveals that care must be taken when comparing external measures of tumor aggressiveness because the behavior, growth, and clinical survival of mice with Ang1 upregulated tumors will be affected by hydrocephalus.

Micro-CT

Finally, we used MRI to select an appropriate tumor-bearing mouse for detailed micro-CT to test this novel approach for visualizing and analyzing brain tumor vasculature. The micro-CT technique produces high-resolution 3D images with 20-μm isotropic voxels of the distribution of a blood contrast agent in the excised brain from a mouse. Figure 5 shows an example of a slice from the T1-weighted scan in the mouse and the surface-rendered vasculature of the mouse from the micro-CT data, demonstrating good visual agreement of the lesions between the two modalities. This image highlights potential future areas of research and study using micro-CT. We can generate high-resolution 3D images of brain and tumor vasculature and those data sets can be registered to MRI images of the mouse brain using computer software to help interpret how the underlying vascular structure contributes to contrast mechanisms in tumors.

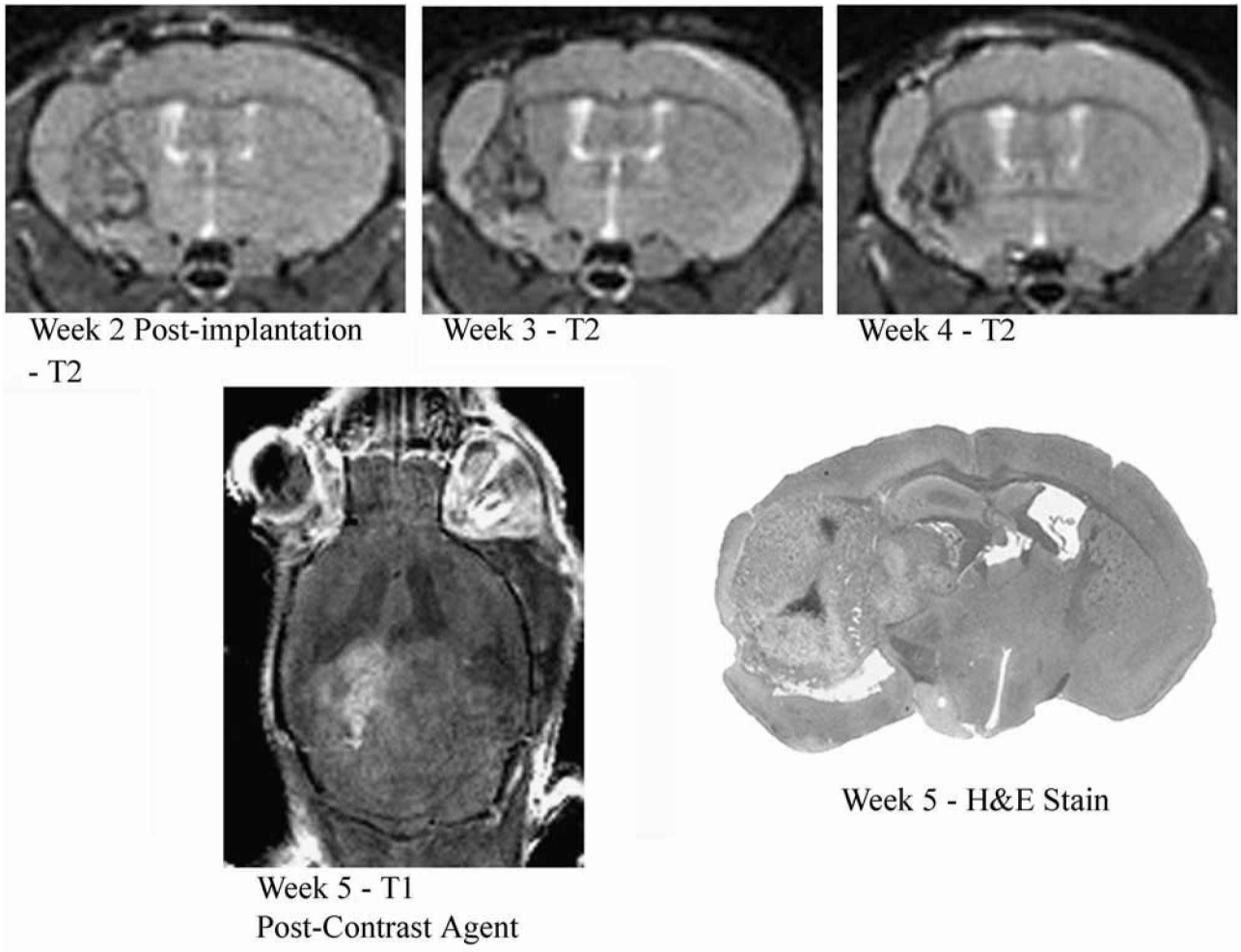

Figure 1. *A time course of MRI images in a single U87 control mouse. The in-plane resolution of MRI images is 156 μm and the slices are 500 μm thick. One slice from the 3D data set for each time point is shown as well as a slide from histology that confirms the presence of a tumor at the final time point.*

Discussion

In this study, we successfully identified tumors in the four groups of mice over the course of their survival using both T2- and T1-weighted images. The early T2-weighted images showed lesions that were predominantly hypointense, with minimal heterogeneity seen in the signal. The hypointense T2 lesions seen in this study are most likely related to the specific characteristics of U87 tumors implanted in mice and the image characteristics will most likely vary with the tumor cell line used to generate orthotopic intracranial xenografts. A recent study [5] shows hyperintense T2 lesions as opposed to the predominantly hypointense lesions we saw, and this highlights the need for further investigation and characterization of individual cell lines used in experimental studies and for understanding the underlying mechanisms of variability in MRI appearance between different intracranial xenograft models to allow accurate and valuable incorporation of MRI images as a routine research modality. We have histologically confirmed the presence of tumors in the location of hypointense T2 lesions seen at week 2 in all mice. The T2-weighted images were also useful for detecting and following the additional unpredicted pathology of hydrocephalus in mice with Ang1 upregulated tumors.

T1 weighting with the contrast agent injection produced good contrast at later time points that corresponded with conventional methods of identifying vascular regions of tumors. Because the mice tolerated the screening well, we will extend the imaging time in future screens and studies so that we can image with both T1 and T2 weighting at each time point. Because T1 weighting requires an injection of contrast agent for each week, we are exploring a method of catheterization [12] or an intraperitoneal injection of contrast agent [13]. Our first ever micro-CT image of mouse intracranial tumor vasculature (Figure 5) shows promise for this technique as a research tool to compliment present methods of analyzing tumor vascularity.

One major finding in this study was that despite established and standardized stereotactic methods of intracranial glioma cell implantation, there was a marked variability in the extent and pattern of tumor growth (Figure 3). Variability is an important finding as it sheds light on the pattern of cell invasion and has implications for use of the model for

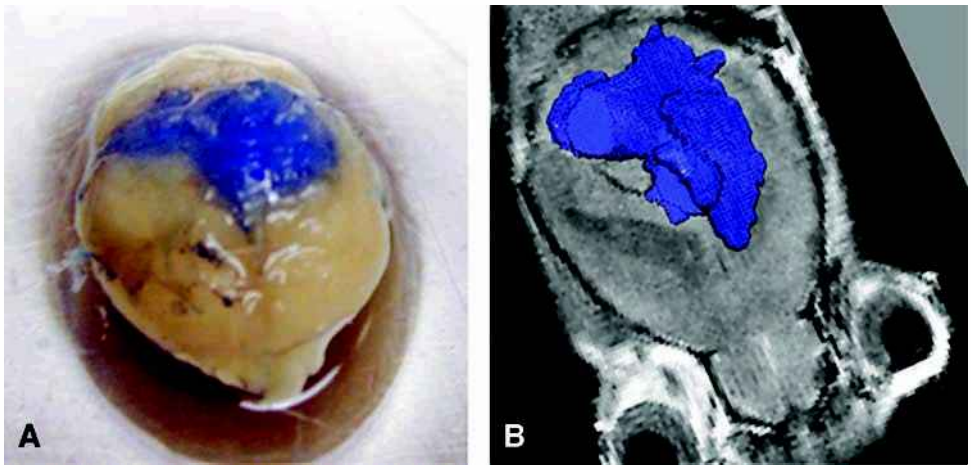

Figure 2. *(A) A photograph of the excised brain from a mouse stained for tumor vasculature with Evans Blue dye. (B) A 3D T1-weighted MRI image from the same mouse before it was sacrificed with a volume-rendered region of contrast enhancement.*

therapeutic studies. The variability in tumor growth, however, means that it is difficult to construct statistically meaningful growth rate curves using a small cohort of mice. From this study, we can conclude that larger numbers of mice have to be included in MRI screens to overcome the high degree of variability in tumor growth and to statistically analyze and

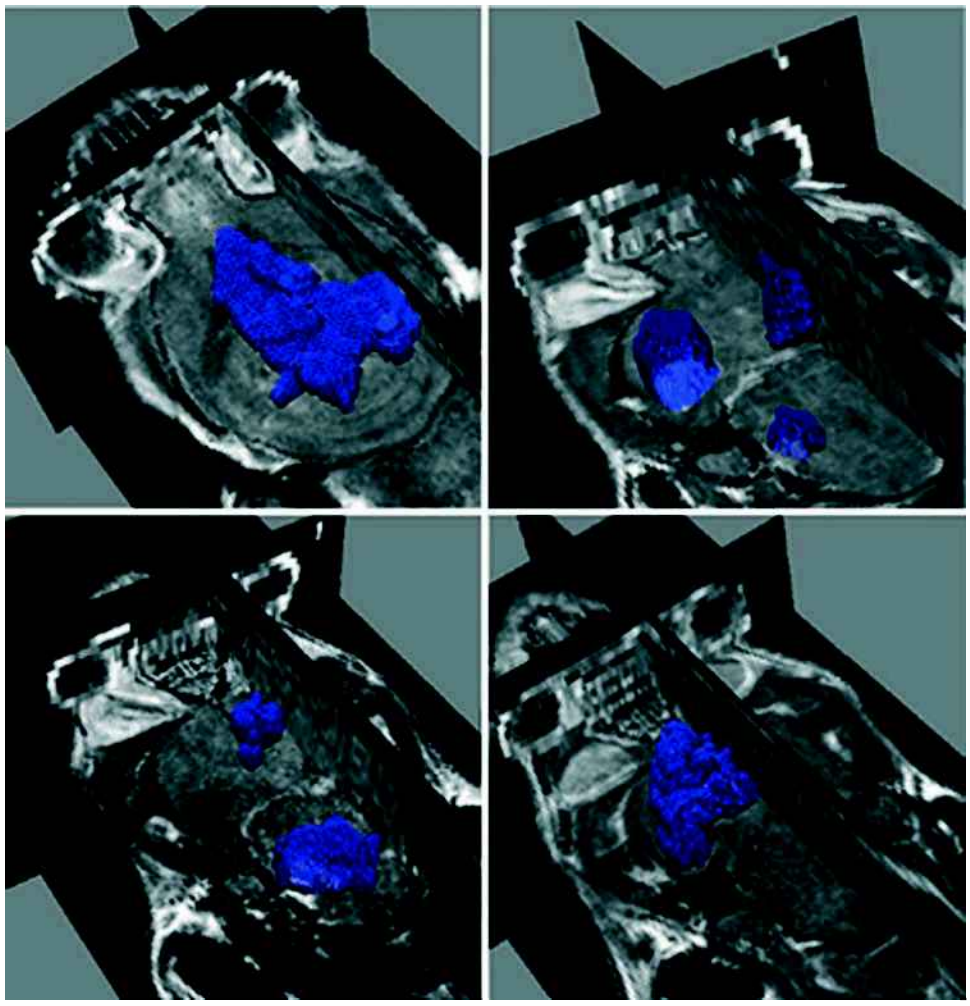

Figure 3. *Volume-rendered regions of enhancement on 3D T1-weighted images of four tumor-bearing mice imaged together at the same time point 5 weeks postinjection.*

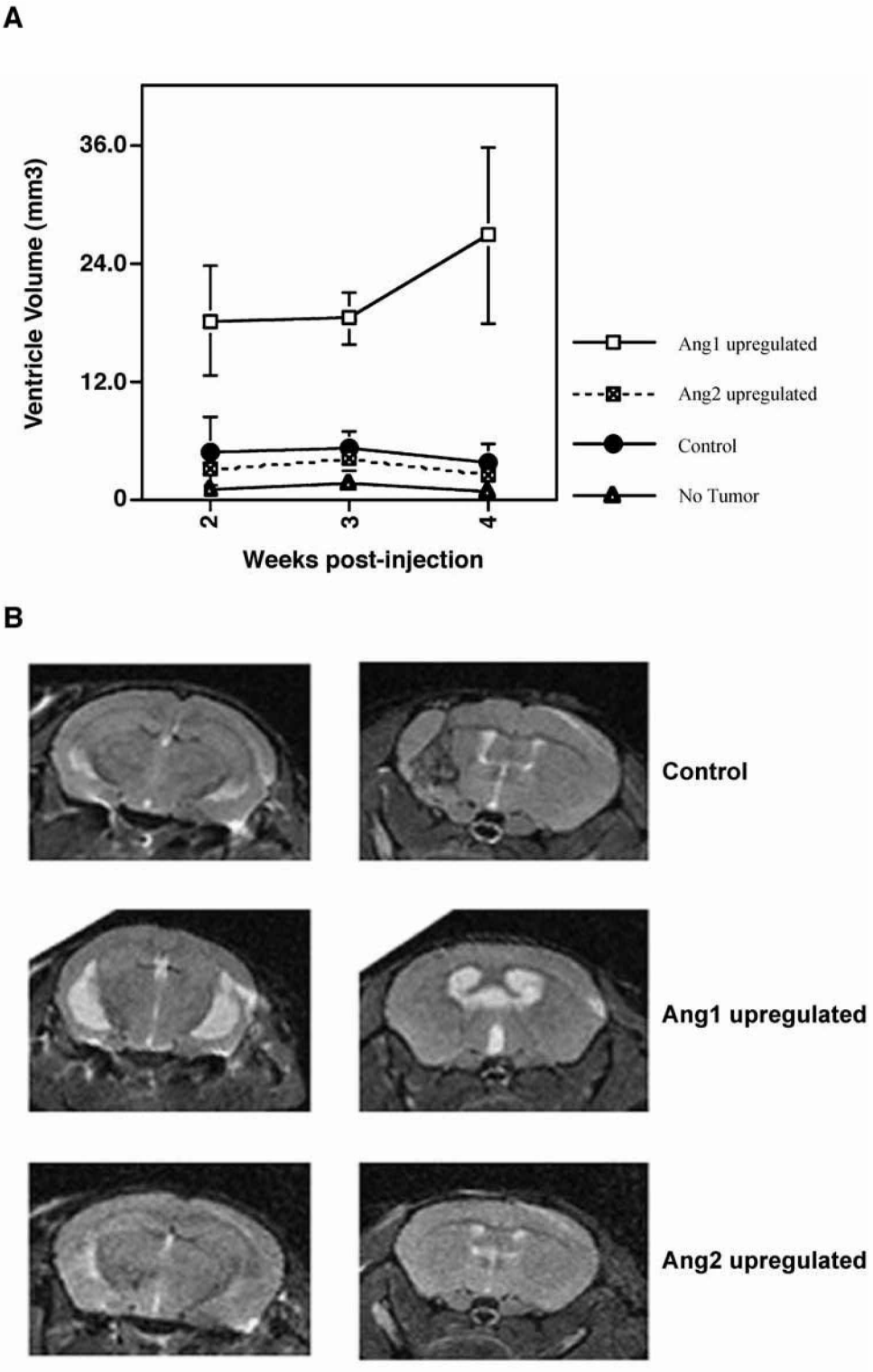

Figure 4. *(A) Ventricle size over time in four groups of age- and sex-matched NODSCID mice (n = 4) measured from T2-weighted MRI images. The ventricles in each 3D data set were manually segmented with in-house image analysis software and their volumes were calculated. (B) Representative images from two slices from each group of mice.*

compare tumor growth rates between different groups of mice. Additionally, in this study, we were unable to accurately interpret tumor volume changes between control, Ang1 and Ang2 tumor groups because the T2-weighted sequences used at earlier time points in the study did not provide precise tumor delineation. Overall, based on this pilot study for future studies, both T1- and T2-weighted sequences should be undertaken at each time point.

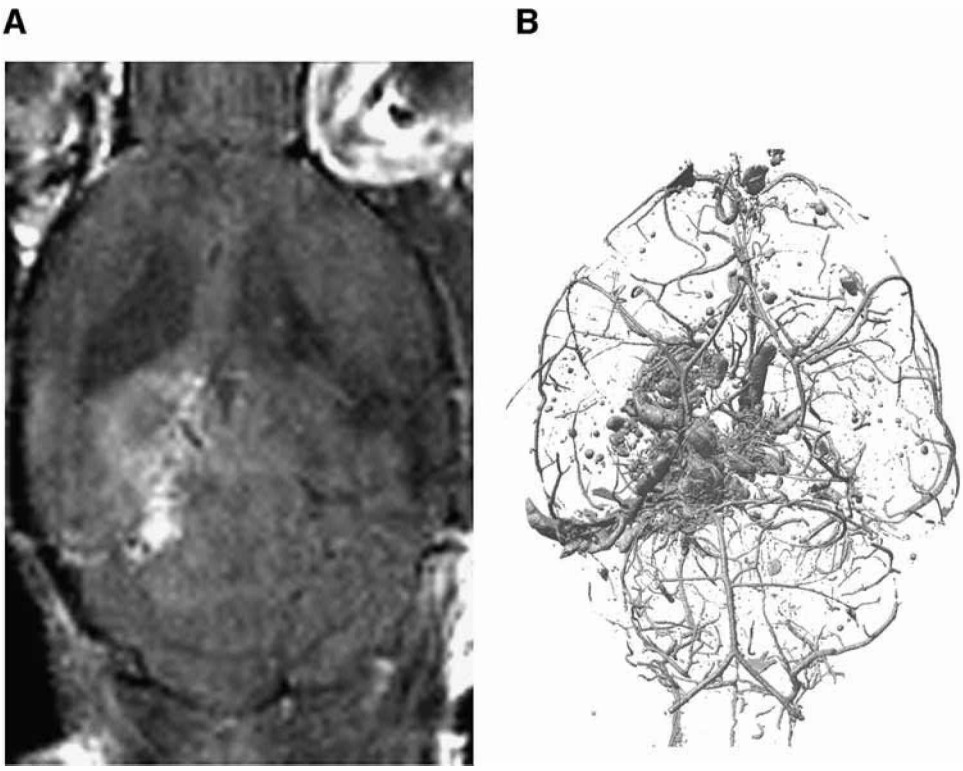

Figure 5. *A slice from a T1-weighted MRI image following an injection of a contrast agent, and the surface-rendered micro-CT image of the vasculature from the excised brain of the same mouse.*

In an attempt to address the issue of larger numbers of mice being imaged by MRI in a reasonable time frame, we increased throughput in this study by a factor of four using our multiple-mouse technique. To date, there has been only one study by Xu et al. [14] that has also demonstrated a multiple-mouse screening technique; however, the low sensitivity in their experiment from using a single large radio-frequency coil loaded with many mice meant that the imaging was only suitable for detecting late tumors just before they were large enough to impact the physiological functions of the mice. Nelson et al. [11] and Cha et al. [3] have both recently shown the excellent sensitivity of single-mouse high-field MRI for screening and following tumors from a much earlier stage of development. The advantage of our multiple-mouse technique is that it produces similar high-quality images but with a much higher throughput.

The results of this study suggest that a useful MRI screen for intracranial tumor models consists of weekly high-resolution 3D whole brain imaging with T2 and T1 weighting with contrast agent injection using a high-field multiple-mouse MRI system. Although this might not be a universal screen for all transgenic and xenograft tumor models (the MRI might not be sensitive to some tumors), it provides a thorough and simple approach to longitudinal screening. We have demonstrated that longitudinal weekly MRI is a feasible method of following tumor growth and believe that it should be a major research tool for studying intracranial tumor biology in both xenograft and transgenic mouse models.

Acknowledgements

We thank the National Cancer Institute of Canada, Canadian Institutes of Health Research, Canada Foundation for Innovation, Ontario Research and Development Challenge Fund, Natural Sciences and Engineering Research Council of Canada for grant support.

References

[1] Weiss WA, Israel M, Cobbs C, Holland E, James CD, Louis DN, Marks AI, McClatchey AI, Roberts T, Van Dyke T, Wetmore C, Chiu IM, Giovannini M, Guha A, Higgins RJ, Marino S, Radovanovic I, Reilly K, and Aldape K (2002). Neuropathology of genetically engineered mice: consensus report and recommendations from an international forum. *Oncogene* **21** (49), 7453–463.

[2] Adzamli K, Yablonskiy DA, Chicoine MR, Won EK, Galen KP, Zahner TA, Woolsey TA, and Ackerman JJ (2003). Albumin-binding MR blood pool agents as MRI contrast agents in an intracranial mouse glioma model. *Magn Reson Med* **49** (3), 586–90.

[3] Cha S, Johnson G, Wadghiri YZ, Jin O, Babb J, Zagzag D, and Turnbull DH (2003). Dynamic, contrast-enhanced perfusion MRI in mouse gliomas: correlation with histopathology. *Magn Reson Med* **49** (5), 848–55.

[4] Poptani H, Duvvuri U, Miller CG, Mancuso A, Charagundla S, Fraser JD, Glickson JD, Leigh JS, and Reddy R (2001). T1rho imaging of murine brain tumors at 4 T. *Acad Radiol* **8** (1), 42–47.

[5] Tada T, Wendland M, Watson N, Kuriyama N, Kuriyama H, Roberts M, Burns M, Weiss W, and Israel MA (2002). A head holder for magnetic resonance imaging that allows the stereotaxic alignment of spontaneously occurring intracranial mouse tumors. *J Neurosci Methods* **116** (1), 1–7.

[6] Bock NA, Konyer NB, and Henkelman RM (2003). Multiple-mouse MRI. *Magn Reson Med* **49** (1), 158–67.

[7] Wong WH, and Sukumar, S (2000). Millipede imaging coil design for

high field micro imaging applications. *Proceedings of the ISMRM 8th Annual Meeting*, 1399.

[8] Guilfoyle DN, Dyakin VV, O'Shea J, Pell GS, and Helpern JA (2003). Quantitative measurements of proton spin–lattice (T1) and spin–spin (T2) relaxation times in the mouse brain at 7.0 T. *Magn Reson Med* **49** (3), 576–80.

[9] Feldkamp LA, and Kress, JW (1984). Practical cone-beam algorithm. *J Opt Soc Am* **1** (6), 612–19.

[10] Ma HI, Guo P, Li J, Lin SZ, Chiang YH, Xiao X, and Cheng SY (2002). Suppression of intracranial human glioma growth after intramuscular administration of an adeno-associated viral vector expressing angiostatin. *Cancer Res* **62** (3), 756–63.

[11] Nelson AL, Algon SA, Munasinghe J, Graves O, Goumnerova L, Burstein D, Pomeroy SL, and Kim JY (2003). Magnetic resonance imaging of patched heterozygous and xenografted mouse brain tumors. *J Neuro-Oncol* **62** (3), 259–67.

[12] Koutcher JA, Hu X, Xu S, Gade TP, Leeds N, Zhou XJ, Zagzag D, and Holland EC (2002). MRI of mouse models for gliomas shows similarities to humans and can be used to identify mice for preclinical trials. *Neoplasia* **4** (6), 480–85.

[13] Taillandier L, Antunes L, and Angioi-Duprez KS (2003). Models for neuro-oncological preclinical studies: solid orthotopic and heterotopic grafts of human gliomas into nude mice. *J Neurosci Methods* **125** (1–2), 147–57.

[14] Xu S, Gade TP, Matei C, Zakian K, Alfieri AA, Hu X, Holland EC, Soghomonian S, Tjuvajev J, Ballon D, and Koutcher JA (2003). *In vivo* multiple-mouse imaging at 1.5 T. *Magn Reson Med* **49** (3), 551–57.